Int. J. Heat Mass Transfer. Vol. 33, No. 6, pp. 1087–1097, 1990
Printed in Great Britain

0017–9310/90 $3.00 + 0.00

Numerical determination of wall functions for the turbulent natural convection boundary layer

R. A. W. M. HENKES and C. J. HOOGENDOORN
Department of Applied Physics, Delft University of Technology, P.O. Box 5046, 2600 GA Delft, The Netherlands

(*Received* 21 *February* 1989)

Abstract—In an analytical way George and Capp (*Int. J. Heat Mass Transfer* **22**, 813–826 (1979)) and Cheesewright ("The scaling of turbulent natural convection boundary layers in the asymptotic limit of infinite Grashof number", paper presented at Euromech Colloquium 207 (1986)) have derived wall functions for the natural convection boundary layer along a heated vertical plate. These wall functions are compared here with numerical calculations for air, using a k–ε turbulence model with low-Reynolds number modifications. George and Capp's wall function for the temperature in the inner layer agrees with the calculations, but their wall function for the velocity does not. George and Capp's defect laws for the velocity and the temperature in the outer layer are also numerically found, but Cheesewright's wall function for the velocity in the (lower part of the) outer layer does not agree.

1. INTRODUCTION

A LARGE part of the velocity profile of the turbulent boundary layer along a flat plate placed in an oncoming flow can be described by a logarithmic wall function. Most numerical calculations of turbulent flows use this wall function as a boundary condition. In this way the use of many computational grid points to describe the steep gradients in the turbulent flow close to a fixed wall can be avoided. The logarithmic wall function only approximately holds for forced convection boundary layers with small pressure gradients; it does not hold for natural convection boundary layers. In an analytical way George and Capp [1] and Cheesewright and Mirzai [2, 3] have given some ideas about the wall functions for the natural convection boundary layer along a heated vertical plate.

George and Capp divided the boundary layer into an inner and outer layer. The inner layer starts at the wall and ends at the velocity maximum. This layer is further split in a conductive/thermo-viscous sublayer, directly touching the wall, and in a buoyant sublayer extending to the velocity maximum. A 1/3-power wall function for the velocity and a $-1/3$-power wall function for the temperature is proposed in this buoyant sublayer. A defect law is given in the outer layer, which extends from the velocity maximum up to the outer edge.

Cheesewright's analysis differs from that of George and Capp on some points. The form of the flow in the conductive/thermo-viscous sublayer remains unchanged. Cheesewright derived wall functions in the lower part of the outer layer (i.e. the fully turbulent region between the maxima of the velocity and the turbulent viscosity). These wall functions do not show the 1/3-power dependence, but have logarithmic terms. He did not formulate a defect law in the upper part of the outer layer.

This paper compares the proposed wall functions with existing experimental data and new numerical data for air.

An important contribution to the experimental knowledge of the natural convection boundary layer has recently been given by Tsuji and Nagano [4]. They accurately measured the velocity very close to the wall. With the help of these data and the velocity and temperature data of others [2, 3, 5–10] we will verify the accuracy of the numerical results. The numerical results are obtained by solving the boundary-layer equations along the heated vertical plate. The turbulence is modelled with a low-Reynolds number k–ε model. Several low-Reynolds number k–ε turbulence models are considered. Once we are convinced that the numerical model works well for the Grashof numbers for which experiments are available, we also expect the model to be accurate for higher Grashof numbers.

Calculations are performed for air (Prandtl number 0.71) up to a local Grashof number of 10^{12}. This enables us to study the asymptotic structure (i.e. the large Grashof number behaviour) of the turbulent natural convection boundary layer. The following quantities are examined for increasing Grashof number: wall-heat transfer, wall-shear stress, the velocity maximum and its position, and the maximum of the turbulent viscosity and its position. All these quantities approximately show an asymptotic behaviour of the form αGr_x^{γ}. The power γ turns out to be almost independent of the model used, but the proportionality coefficient α shows a larger model dependence. The asymptotic behaviour of the different quantities is related to possible similarity scalings (i.e.

NOMENCLATURE

c_{fx}	dimensionless wall-shear stress, $2\nu(\partial u/\partial y)_w/u_b^2$
g	gravitational acceleration
Gr_x	local Grashof number, $g\beta\Delta T x^3/\nu^2$
k	turbulent kinetic energy
Nu_x	local Nusselt number, $-(x/\Delta T)[\partial(T-T_\infty)/\partial y]_w$
p	pressure
Pr	Prandtl number
Q_T	velocity scale, $-(\nu/(Pr\,\Delta T))(\partial T/\partial y)_w$
Re_x	local Reynolds number, $u_\infty x/\nu$
T	temperature
ΔT	characteristic temperature difference, T_w-T_∞
u	velocity component along the plate
u_0	velocity scale, $(g\beta\Delta T\nu)^{1/3}$
u_b	velocity scale, $\sqrt{(g\beta\Delta T x)}$
u_τ	velocity scale, $\sqrt{(\nu(\partial u/\partial y)_w)}$
v	velocity component perpendicular to the plate
x	coordinate along the plate, beginning at the leading edge
y	coordinate perpendicular to, and beginning at, the plate
y^+	dimensionless length, yu_τ/ν.

Greek symbols

β	coefficient of thermal expansion
δ	length scale
ε	rate of dissipation of k
ζ	dimensionless length, $(yQ_T\,Pr)/\nu = (y\,Nu_x)/x$
λ	dimensionless length, $Gr_y^{1/3}$
ν	molecular kinematic viscosity
ν_t	turbulent kinematic viscosity
ρ	density
σ_T	turbulent Prandtl number for T.

Superscripts

i	inner layer
o	outer layer.

Subscripts

max	maximum of a quantity
w	wall condition
∞	environment condition.

scalings for the temperature, velocity and length that lead to solutions that are independent of the Grashof number). In order to check that these scalings indeed lead to similarity solutions (wall functions, defect laws) we have plotted calculated velocity and temperature profiles for increasing Grashof number. We have also plotted the similarity profiles for the turbulent quantities: the turbulent viscosity, the kinetic energy of the turbulence and the rate of turbulent energy dissipation.

We also give some reflections about the possibilities of practical use of wall functions in natural convection calculations.

2. SIMILARITY SCALINGS

The boundary-layer flow along a fixed wall can be described by the boundary-layer equations. For a turbulent, two-dimensional, incompressible, Boussinesq flow these equations read

$$\frac{\partial u}{\partial x}+\frac{\partial v}{\partial y}=0$$

$$\frac{\partial u^2}{\partial x}+\frac{\partial uv}{\partial y}=-\frac{1}{\rho}\frac{\mathrm{d}p}{\mathrm{d}x}+g\beta(T-T_\infty)+\frac{\partial}{\partial y}(\nu+\nu_t)\frac{\partial u}{\partial y}$$

$$\frac{\partial uT}{\partial x}+\frac{\partial vT}{\partial y}=\frac{\partial}{\partial y}\left(\frac{\nu}{Pr}+\frac{\nu_t}{\sigma_T}\right)\frac{\partial T}{\partial y} \qquad (1)$$

with the boundary conditions

$$x=x_b:\quad u\text{- and } T\text{-profile prescribed}$$

$$y=0:\quad u=v=0,\quad T=T_w$$

$$y\to\infty:\quad u=u_\infty,\quad T=T_\infty=T_w-\Delta T.$$

Here x is the coordinate along the plate. The solution of these equations for a forced convection flow (constant, non-zero u_∞) only depends on the Prandtl number (Pr) and on the x-based Reynolds number ($Re_x=u_\infty x/\nu$). The natural convection solution ($u_\infty=0$) only depends on Pr and on the x-based Grashof number ($Gr_x=g\beta\Delta T x^3/\nu^2$). Hence, for a fixed Prandtl number we have

$$\frac{u}{(g\beta\Delta T\nu)^{1/3}}=f_u\left(Gr_x,\frac{y}{x}\right)$$

$$\frac{T-T_\infty}{\Delta T}=f_T\left(Gr_x,\frac{y}{x}\right). \qquad (2)$$

If the characteristic number (Gr_x or Re_x) becomes infinitely large, a rescaling might exist, which makes the solution independent of this characteristic number. In general, such a similarity solution is described by

$$\frac{u}{(g\beta\Delta T\nu)^{1/3}}f_1(Gr_x)=f_2\left(\frac{y}{x}f_3(Gr_x)\right)$$

$$\frac{T-T_\infty}{\Delta T}f_4(Gr_x)=f_5\left(\frac{y}{x}f_6(Gr_x)\right). \qquad (3)$$

For a laminar flow the similarity scalings are well known [11], namely with $f_1=Gr_x^{-1/6}$, $f_3=f_6=Gr_x^{1/4}$

and $f_4 = 1$. The laminar velocity scale $(g\beta\Delta Tv)^{1/3} \times Gr_x^{1/6}$ $(= \sqrt{(g\beta\Delta Tx)})$ is here further referred to as u_b (buoyant velocity). The velocity $(g\beta\Delta Tv)^{1/3}$ is indicated as u_0. The similarity scalings for the turbulent boundary layer are more complicated. In particular this is because for large Gr_x (or Re_x) the solution across the boundary layer is split in several regions, where different scalings hold. For a forced convection turbulent boundary layer these scalings are well known (see, e.g. Cebeci and Bradshaw [12]) : a viscous sublayer close to the wall, an inertial sublayer where the logarithmic wall function holds, and an outer layer at the edge of the boundary layer where a defect law holds. Some first steps to detect the different regions and scalings in the turbulent natural convection boundary layer were made by George and Capp [1] and by Cheesewright and Mirzai [2, 3]. The main steps of their analyses are summarized here for a fixed Prandtl number.

George and Capp assumed that the length scale δ and the velocity scales u_τ and Q_T were important for the scaling

$$\delta = \text{boundary-layer thickness}$$

$$u_\tau = \sqrt{(\nu(\partial u/\partial y)_w)}$$

$$Q_T = -\frac{\nu}{Pr\,\Delta T}\left(\frac{\partial T}{\partial y}\right). \tag{4}$$

In general (with $u_0 = (g\beta\Delta T\nu)^{1/3}$)

$$\frac{u}{u_0} = f_u(\zeta, y^+, \lambda, y/\delta, Gr_x^{1/3})$$

$$\frac{T-T_\infty}{\Delta T} = f_T(\zeta, y^+, \lambda, y/\delta, Gr_x^{1/3}) \tag{5}$$

with the five dimensionless lengths

$$\zeta = \frac{yQ_T}{\nu/Pr}$$

$$y^+ = \frac{yu_\tau}{\nu}$$

$$\lambda = \left(\frac{g\beta\Delta T}{\nu^2}\right)^{1/3} y = Gr_y^{1/3}$$

$$y/\delta$$

$$Gr_x^{1/3} = \left(\frac{g\beta\Delta Tx^3}{\nu^2}\right)^{1/3}.$$

In the inner layer the dependence on y/δ is neglected. Moreover, a local equilibrium state is assumed in this layer; in that case only u_τ/u_0 and Q_T/u_0 depend on Gr_x and the explicit dependence on Gr_x can be removed from expressions (5). If it is further assumed that there is only one length scale in the inner layer (i.e. $\zeta \div \lambda$ and $y^+ \div \lambda$) u_τ/u_0 and Q_T/u_0 are even independent of Gr_x. Under these assumptions the wall-shear stress law (with $c_{fx} = 2\nu(\partial u/\partial y)_w/u_b^2$ and the wall-heat transfer law $(Nu_x = -(x/\Delta T)[\partial(T-T_\infty)/\partial y]_w$) read

$$c_{fx} \div Gr_x^{-1/3} \tag{6a}$$

$$Nu_x \div Gr_x^{1/3}. \tag{6b}$$

In the lower part of the inner layer, the conductive/thermo-viscous sublayer, both convection and turbulence can be neglected. Using series expansions in equations (1) gives

$$\frac{u}{u_0} = \frac{u_\tau^2}{u_0^2}\lambda - \frac{\lambda^2}{2}\left(1 - \frac{\lambda}{3}\frac{Q_T}{u_0}Pr\right) + \cdots \tag{7a}$$

$$\frac{T-T_\infty}{\Delta T} = 1 - \zeta + \cdots. \tag{7b}$$

The assumption of one length scale gives wall functions in the upper part of the inner layer, the buoyant sublayer

$$\frac{u}{u_0} = f_u^i(\zeta)$$

$$\frac{T-T_\infty}{\Delta T} = f_T^i(\zeta). \tag{8}$$

In the outer layer the dependence on y^+, ζ and λ is neglected in expressions (5). In order to remove the Gr_x dependence as well, an equilibrium state is assumed: the velocity scale and temperature scale in the outer layer are assumed to depend on δ, $g\beta$ and $Q_T\Delta T$ only. This gives the following defect laws in the outer layer:

$$\frac{u-u_{max}}{u_0\zeta_\delta^{1/3}} = f_u^o\left(\frac{y}{\delta}\right)$$

$$\left(\frac{T-T_\infty}{\Delta T}\right)\frac{Gr_\delta^{1/3}}{\zeta_\delta^{2/3}} = f_T^o\left(\frac{y}{\delta}\right). \tag{9}$$

Here $\zeta_\delta = (\delta Q_T\ Pr)/\nu$ and $Gr_\delta = g\beta\Delta T\delta^3/\nu^2$. For a smooth matching of the conductive/thermo-viscous sublayer with the outer layer, expressions (8) and (9) must hold in an intermediate layer, the buoyant sublayer. This gives George and Capp's wall functions in the buoyant sublayer

$$\frac{u}{u_0} = c_1\zeta^{1/3} + c_2 \tag{10a}$$

$$\frac{T-T_\infty}{\Delta T} = c_3\zeta^{-1/3} + c_4. \tag{10b}$$

These 1/3- and $-1/3$-power laws in the buoyant sublayer should be the natural convection counterpart of the log-law in the inertial sublayer of the forced convection boundary layer.

Cheesewright has proposed a different wall function. The conductive/thermo-viscous sublayer in his analysis remains, of course, the same as expressions (7). He assumes that relation (8) still holds in the lower part of the outer layer (i.e. the region between the positions of the maxima of the velocity and the turbulent viscosity, see also Section 4) and that there is no dependence on ν, which leads to

$$\frac{T-T_\infty}{\Delta T} = c_0 \ln \zeta + c_1. \tag{11}$$

Neglecting convection and molecular diffusion in equations (1) gives (taking $\sigma_T = 1$)

$$\frac{\partial u}{\partial y} = \frac{u_\tau^2 - g\beta\Delta T \int_0^y \frac{T-T_\infty}{\Delta T}\,dy}{\nu_t}$$

$$\frac{\partial}{\partial y}\left(\frac{T-T_\infty}{\Delta T}\right) = -\frac{Q_T}{\nu_t}. \tag{12}$$

Substitution of equation (11) into equations (12) gives

$$\frac{u}{u_0} = -c_0 \frac{u_0^2}{Pr\,Q_T^2}\left[Pr \frac{u_\tau^2 Q_T}{u_0^3} \ln \zeta - (c_1 - 2c_0)\zeta - c_0 \zeta \ln \zeta \right] + c_3. \tag{13}$$

Cheesewright proposed equations (11) and (13) as wall functions in the lower part of the outer layer. He did not formulate a defect law in the upper part of the outer layer.

3. EXISTING EXPERIMENTAL DATA

Wall-heat transfer measurements for air were obtained by Siebers *et al.* [10], Miyamoto *et al.* [8] and Cheesewright and Ierokipiotis [6]. Comparison of their data leads to the best-fit curve (for air)

$$Nu_x = 0.106 Gr_x^{1/3}. \tag{14}$$

Miyamoto *et al.* [9] measured velocity and temperature profiles for air in the boundary layer along a vertical plate with a constant wall-heat flux. Because Nu_x/x is (approximately) independent of x according to equation (14), these measurements are also valid for the vertical plate with constant wall temperature. Cheesewright and co-workers [2, 5–7] and Tsuji and Nagano [4] measured velocity and temperature profiles for air along a vertical plate with constant wall temperature. Measured velocity and temperature profiles are plotted in Fig. 1. We note that the profiles for different Gr_x are only expected to coincide if the quantities are non-dimensionalized with the right scalings. The measured temperature profiles almost coincide, but the deviation between the velocity profiles is larger.

Tsuji and Nagano [4] were able to measure the velocity very close to the wall, leading to the following best-fit curve for the wall-shear stress

$$c_{fx} = 1.368 Gr_x^{-0.249}. \tag{15}$$

The wall-shear stress data of Cheesewright and Mirzai [3] are more scattered, but they derived a best-fit curve with a power dependence close to equation (15), namely $c_{fx} = 2Gr_x^{-0.26}$.

It is difficult to judge the accuracy of the measurements. It has to be realized that the experimental

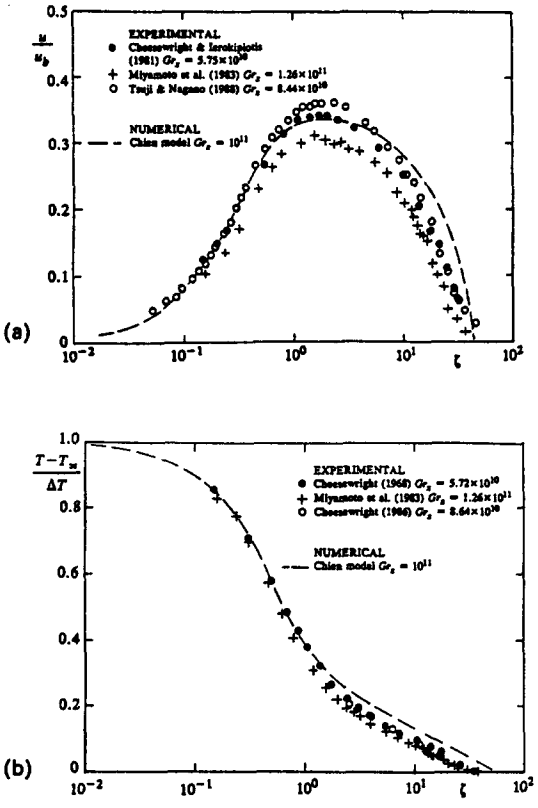

FIG. 1. Comparison between measured and calculated profiles: (a) velocity; (b) temperature.

situation is never the semi-infinite vertical plate in an infinitely large, isothermal environment. The plate is placed in a box with finite dimensions, introducing a temperature stratification along the outer edge of the boundary layer. Tsuji and Nagano [4] suggested that their measurements have a good accuracy, because they used a hot-wire technique. The other experiments mentioned all used laser-Doppler anemometry; this technique seems to give a too large measuring volume close to the wall, leading to inaccurate results in the near-wall region.

The relevance of the wall functions summarized in the preceding section is difficult to check on the grounds of the existing experimental data alone. In particular the experiments are restricted to $Gr_x = 2 \times 10^{11}$, which might be too low for the asymptotic scaling laws to appear. Therefore, the details of the natural convection boundary layer up to $Gr_x = 10^{12}$ are examined with a numerical model.

4. NUMERICAL RESULTS

The wall functions are compared with the numerical solution of the turbulent natural convection boundary-layer equations (1). The turbulence models and numerical procedure are described in detail in ref. [13]. The numerical calculations are performed with a low-Reynolds number k–ε model for turbulence. Different models were tested, and the models of Jones and

Launder [14], Chien [15, 16] and Lam and Bremhorst [17] turned out to give the best wall-heat transfer results. These best models are used here. Although leading to a too high wall-heat transfer, we will also give the results for the standard k–ε model (i.e. without low-Reynolds number modifications), because this model is still most commonly used in numerical calculations.

The boundary-layer flow for air along a heated vertical plate was calculated in the Gr_x range 10^9–10^{12}, using the Boussinesq approximation. The calculation

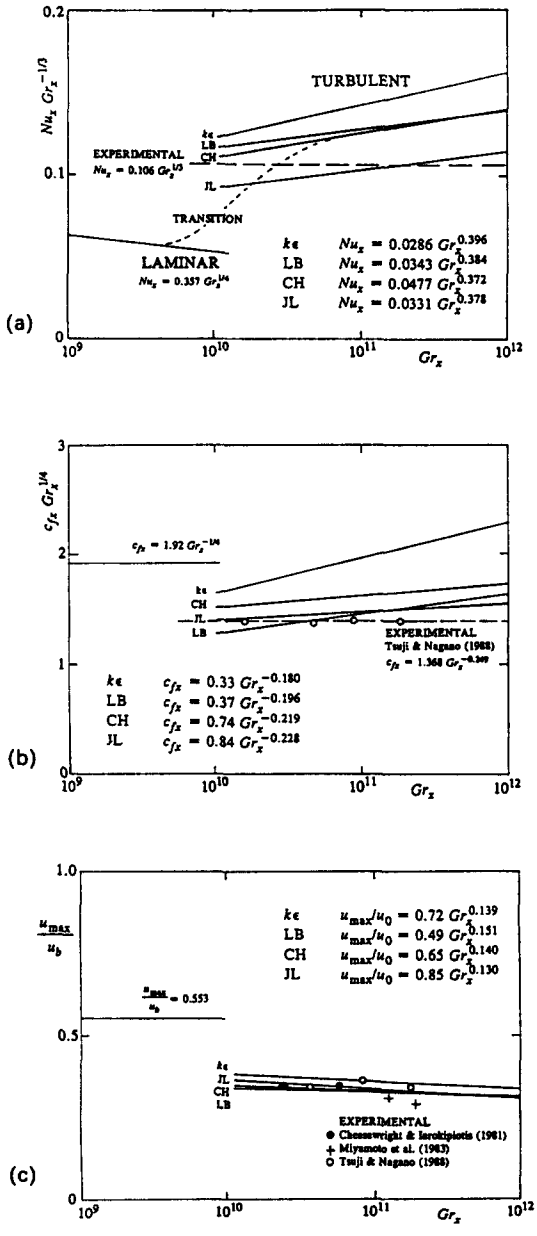

FIG. 2. Turbulent asymptotic behaviour of different quantities: (a) wall-heat transfer; (b) wall-shear stress; (c) velocity maximum; (d) position of the velocity maximum; (e) turbulent viscosity maximum; (f) position of the turbulent viscosity maximum. $k\varepsilon$, standard k–ε model; LB, Lam and Bremhorst model; CH, Chien model; JL, Jones and Launder model.

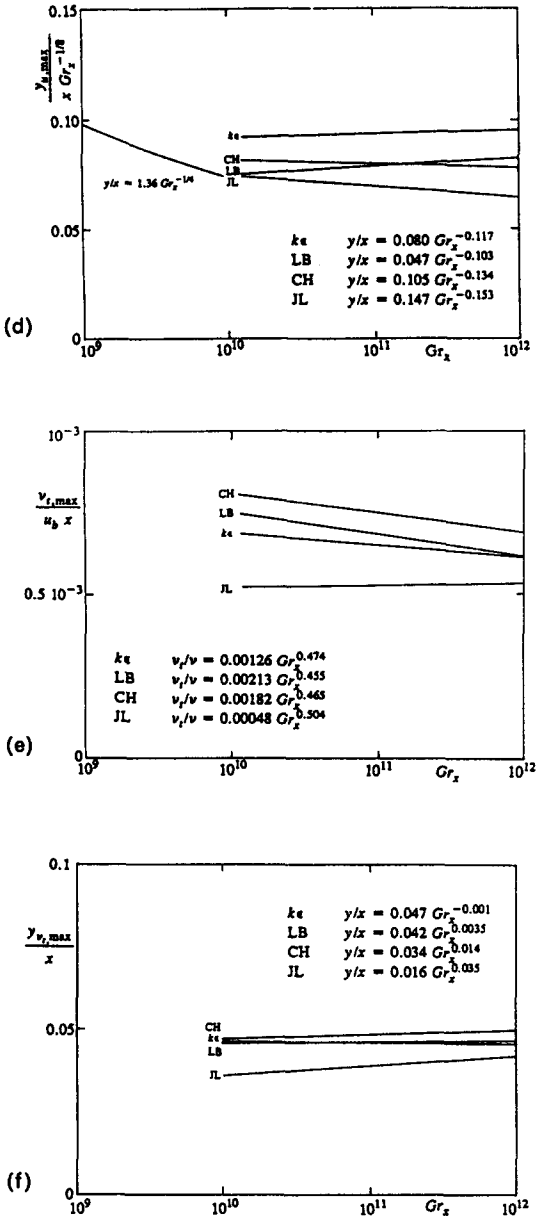

FIG. 2.—*Continued.*

was started with the laminar solution at $Gr_x = 10^9$, and an amount of turbulent kinetic energy was introduced at $Gr_x = 2 \times 10^9$ to obtain a transition to the turbulent solution.

Figure 1 shows that the Chien model closely predicts the experimental velocity and temperature profiles in the range up to $Gr_x \sim 2 \times 10^{11}$ (see also Figs. 2(a)–(c)). As discussed in ref. [13] the models of Jones and Launder, Lam and Bremhorst and (to some extent) the standard k–ε model closely calculate these profiles also. Because the models work well in the experimental Grashof number range, it is reasonable to expect that they also give good predictions for higher Grashof numbers, where no experimental data are available. The numerical results for these larger Grashof numbers will be used to derive wall functions.

The calculated Gr_x dependence of the wall-heat transfer, the wall-shear stress, the velocity maximum and its position, and the maximum of the turbulent viscosity and its position are shown in Fig. 2. The transition from the laminar asymptote to the turbulent asymptote largely depends on the turbulence model used. This transition is illustrated for the Chien model in Fig. 2(a). The turbulent solution between $Gr_x = 10^{11}$ and 10^{12} is fitted to an asymptotic curve of the form αGr_x^{γ} with a least-squares numerical method. These fitted curves are shown in Fig. 2. We suggest that these curves are asymptotic, but we only checked it up to $Gr_x = 10^{12}$. All the turbulence models approximately give the same Gr_x power dependencies, namely

$$\begin{aligned} Nu_x &\div Gr_x^{1/3} \\ c_{fx} &\div Gr_x^{-1/4} \\ u_{\max} &\div u_0\, Gr_x^{1/6} (= u_b) \\ y_{u,\max} &\div x\, Gr_x^{-1/8} \\ \nu_{t,\max} &\div \nu\, Gr_x^{1/2} (= u_b x) \\ y_{\nu_t,\max} &\div x. \end{aligned} \tag{16}$$

The proportionality coefficients show some model dependence. In ref. [13] we concluded that the Jones and Launder model gives the best wall-heat transfer results for air, whereas the standard k–ε model gives a value which is much too high. Comparison with the recent data of Tsuji and Nagano [4] leads to the same conclusion for the wall-shear stress. However, it is important that all the models approximately predict the experimentally found $-1/4$-power dependence in the wall-shear stress and the 1/3-power dependence in the wall-heat transfer. Further, the experiments seem to confirm the numerical result that the velocity maximum approximately scales with u_b.

Now we compare the wall functions as proposed by George and Capp with both the existing experimental data and the new numerical data.

4.1. *Conductive/thermo-viscous sublayer*

Substitution of the experimental relation for the wall-heat transfer (14) and the wall-shear stress (15) into expressions (7) gives (we take the power 0.25 instead of 0.249)

$$\frac{u}{u_b} = 0.684\left(\frac{y}{x}Gr_x^{1/4}\right) - 0.5\left(\frac{y}{x}Gr_x^{1/4}\right)^2 + 0.0177\, Gr_x^{1/12}\left(\frac{y}{x}Gr_x^{1/4}\right)^3 + \cdots$$

$$\frac{T - T_\infty}{\Delta T} = 1 - \zeta + \cdots. \tag{17}$$

The first two terms in the series expansion of the velocity show the laminar velocity and length scale, u_b and $x\, Gr_x^{-1/4}$, respectively. This scaling is slightly disturbed in the third term, having a $Gr_x^{1/12}$ contribution. Because the numerical results also give the $-1/4$-power dependence for the wall-shear stress (Fig. 2(b)), the numerical velocity profiles will also give the laminar scalings for the velocity close to the wall. This is illustrated with the Chien model in Fig. 3(a). The laminar scalings hold until close to the velocity maximum. The wall-shear stress in the formulation of George and Capp (6a) shows a $-1/3$-power dependence on Gr_x, instead of both the experimentally and numerically found value of $-1/4$. Therefore, the velocity in the sublayer of George and Capp does not show the laminar scaling. The 1/3-power dependence on Gr_x of the wall-heat transfer in the model of George and Capp is confirmed by both the experimental and numerical results. Therefore $\zeta \div (y/x)Gr_x^{1/3}$, implying that the temperature in expressions (17) does not show the laminar length scale. The calculated temperature for increasing Gr_x in Fig. 3(b) shows that ζ is the right similarity coordinate until far beyond the velocity maximum.

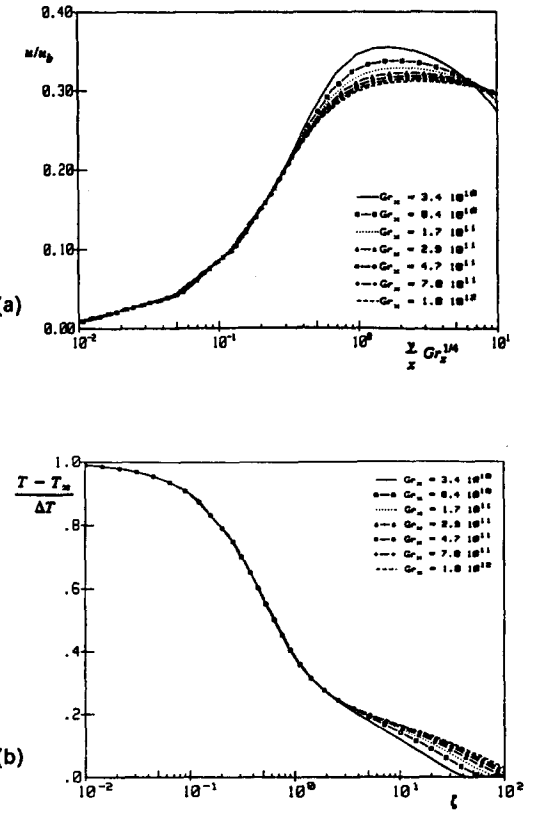

FIG. 3. Calculated similarity profiles in the conductive/thermo-viscous sublayer (Chien model): (a) velocity; (b) temperature.

4.2. *Buoyant sublayer*

This is the layer between the conductive/thermo-viscous sublayer and, say, the position of the velocity maximum. George and Capp proposed the wall function (10a) for the velocity in the buoyant sublayer. As illustrated in Fig. 4(a) indeed both the experiments of

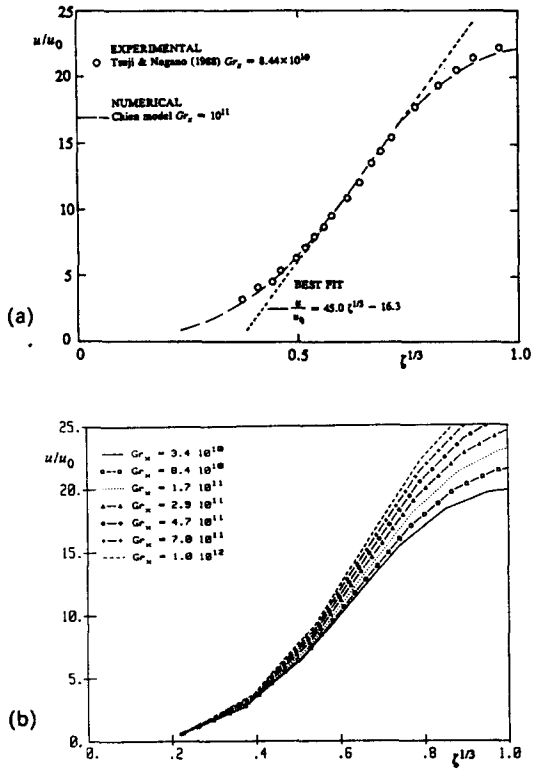

FIG. 4. Velocity in the buoyant sublayer: (a) comparison between experiments and calculations; (b) erroneous similarity scalings (Chien model).

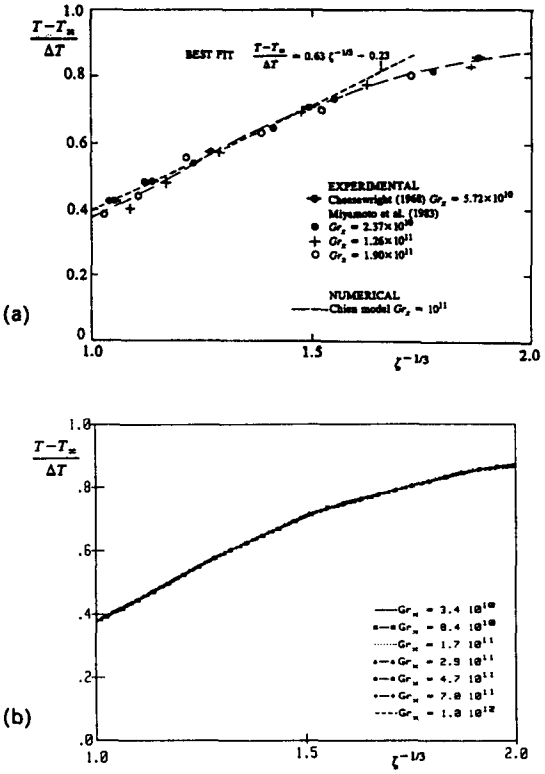

FIG. 5. Temperature in the buoyant sublayer: (a) comparison between experiments and calculations; (b) similarity scalings (Chien model).

Tsuji and Nagano [4] at $Gr_x = 8.44 \times 10^{10}$ and the numerical results at $Gr_x = 10^{11}$ can be fitted to

$$\frac{u}{u_0} = 45\zeta^{1/3} - 16.3. \tag{18}$$

However, the numerical results in Fig. 4(b) for increasing Gr_x show that u/u_0 and ζ are not properly scaled in the buoyant sublayer; the numerical results disagree with George and Capp's velocity wall function. The numerical results in Fig. 3(a) show that the laminar scalings u_b and $x\,Gr_x^{-1/4}$ are the right scalings in the buoyant sublayer. George and Capp proposed the wall function (10b) for the temperature in the buoyant sublayer. As illustrated in Fig. 5(a) both the experiments (in the Gr_x range 2×10^{10}–2×10^{11}) and the numerical results (at $Gr_x = 10^{11}$) can be fitted to

$$\frac{T - T_\infty}{\Delta T} = 0.63\zeta^{-1/3} - 0.23. \tag{19}$$

Moreover, the numerical results for increasing Gr_x in Fig. 5(b) show that plotting $(T - T_\infty)/\Delta T$ vs ζ gives a similarity profile in the buoyant sublayer; the numerical results agree with George and Capp's temperature wall function.

4.3. *Outer layer*

The outer layer extends from the position of the velocity maximum up to the edge of the boundary layer. George and Capp proposed equations (9) as similarity functions (defect laws) in the outer layer. They did not derive how δ/x in the outer layer depends on Gr_x. Our numerical calculations in Fig. 2(f) show that $y_{v_t,\max}/x$ is independent of Gr_x (see expressions (16)). Therefore, if there is indeed one length scale in the outer layer, this implies that also $\delta \div x$. Substitution of $\delta \div x$ and $Nu_x \div Gr_x^{1/3}$ into equations (9) gives

$$\frac{u - u_{\max}}{u_b\, Gr_x^{-1/18}} = f_u^o\left(\frac{y}{x}\right)$$

$$\left(\frac{T - T_\infty}{\Delta T}\right) Gr_x^{1/9} = f_T^o\left(\frac{y}{x}\right). \tag{20}$$

Increasing Gr_x in the numerical Chien model in Fig. 6 shows that both the velocity and temperature are properly scaled in the outer layer by equations (20); the numerical calculations confirm George and Capp's defect laws. George and Capp did not derive how $u_{\max}/u_0$ depends on Gr_x. $u_{\max}$ is positioned between the thermo-viscous sublayer and the outer layer. Therefore, it is expected that the velocity maximum scales with a velocity somewhere between the velocity scaling u_b in the thermo-viscous sublayer and the outer velocity scaling $u_b\, Gr_x^{-1/18}$; say we expect that $u_{\max} \div u_b\, Gr_x^{-1/36}$. In analogy we expect that the position of $u_{\max}$ scales with a length scale between $x\,Gr_x^{-1/4}$ and x; say we expect that

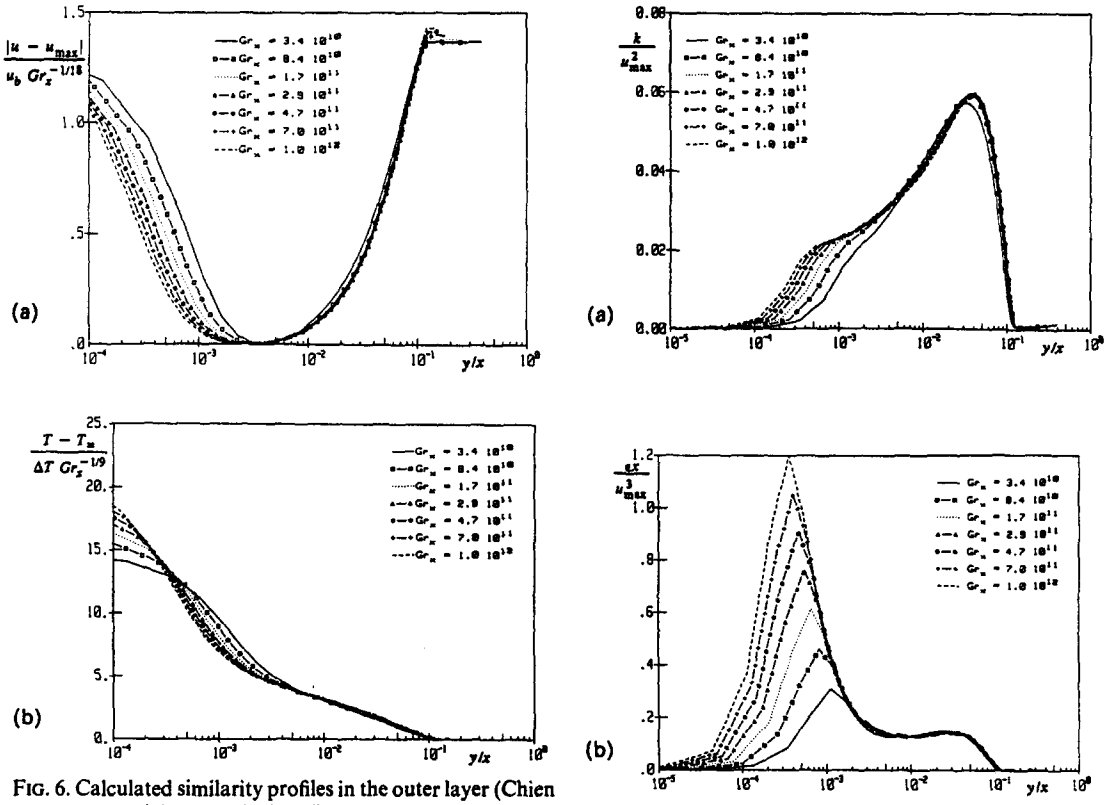

FIG. 6. Calculated similarity profiles in the outer layer (Chien model): (a) velocity; (b) temperature.

$y_{u,\max} \div x\, Gr_x^{-1/8}$. This length scale also approximately follows from the calculations in Fig. 2(d) (see also expressions (16)). But, the expected 1/36-power dependence in the velocity maximum is so small that on the grounds of the numerical calculations in Fig. 3(b) we cannot conclude whether $u_{\max}$ scales with u_b or with $u_b\, Gr_x^{-1/36}$. Moreover, the difference between the outer scaling $u_b\, Gr_x^{-1/18}$ and the laminar velocity scale u_b is small. For example, the use of u_b as the outer velocity scale in Fig. 6(a) only leads to a slightly worse similarity in the outer layer. Because the difference between the velocity scale in the thermo-viscous sublayer, the scaling for the velocity maximum and the outer velocity scale is small, we can conclude that the laminar velocity scale u_b is approximately the right velocity scale over the whole boundary-layer thickness. We checked that scaling the turbulent quantities ν_t, k and ε in the outer layer with the outer velocity scale $u_b\, Gr_x^{-1/18}$ and the outer length scale x approximately leads to similarity profiles. But, the use of $u_{\max}$ as the velocity scale in Fig. 7 leads to the best similarity profiles. Figure 7 shows that the turbulent viscosity is very small up to the position of the velocity maximum. Beyond the position of the velocity maximum the turbulent viscosity grows and reaches a maximum, after which it falls back to zero at the outer edge of the boundary layer.

Cheesewright proposed equation (11) as a wall function for the temperature in the lower part of the outer layer (i.e. the fully turbulent region between the maxima of the velocity and the turbulent viscosity).

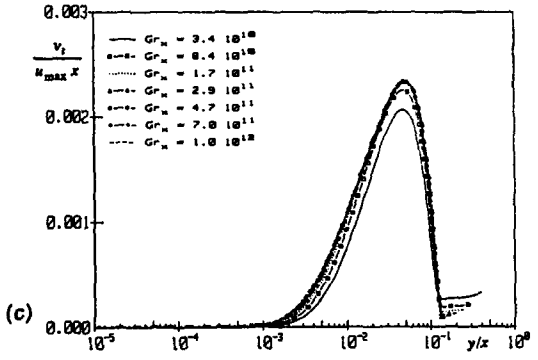

FIG. 7. Calculated similarity profiles for the turbulent quantities in the outer layer: (a) turbulent kinetic energy; (b) rate of turbulent energy dissipation; (c) turbulent viscosity.

He fitted the constants to the experiments (all around $Gr_x \sim 10^{11}$), yielding

$$\frac{T-T_\infty}{\Delta T} = 0.28 - 0.08 \ln \zeta. \qquad (21)$$

This curve is compared with the numerical results for increasing Gr_x in Fig. 8(a). Comparison of the results around $Gr_x \sim 10^{11}$ (see also Fig. 1(b)) shows that the numerical values for the temperature in the lower part of the outer layer are above the experimental values. It is unclear whether this is a shortcoming of the turbulence model or that there was a slight strati-

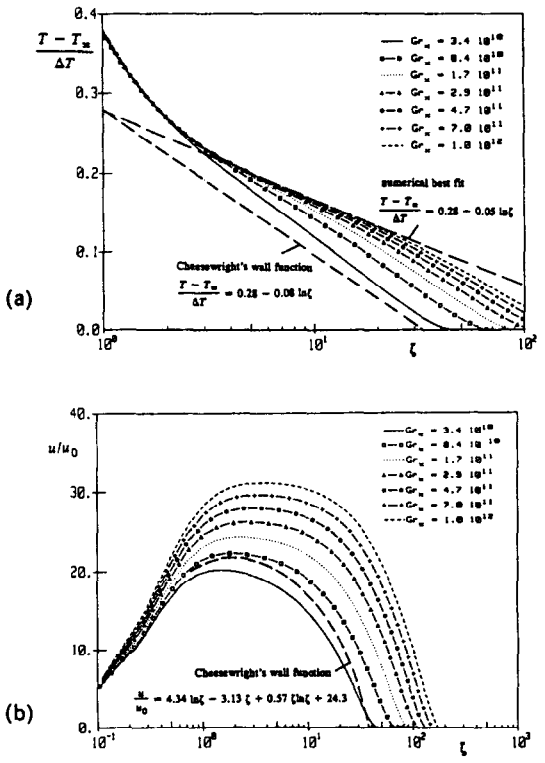

FIG. 8. Cheesewright's wall functions compared with calculations (Chien model): (a) temperature; (b) velocity.

fication in the experiments causing a suppression of the development of the boundary layer. Although not very convincing, the numerical results for large Gr_x in part of the outer layer can be fitted to

$$\frac{T-T_\infty}{\Delta T} = 0.28 - 0.05 \ln \zeta. \tag{22}$$

Hence the numerical results can also be approximately fitted to a logarithmic shape in part of the outer layer, in line with Cheesewright's suggestion. Cheesewright proposed equation (13) as a wall function for the velocity in the lower part of the outer layer. The terms Q_T/u_0 and u_τ/u_0 can depend on Gr_x. The 1/3-power dependence on Gr_x of Nu_x and the $-1/4$-power dependence on Gr_x of c_{fx} imply that Q_T/u_0 actually is independent of Gr_x and $u_\tau/u_0 \div Gr_x^{1/24}$. Hence, except for the last very weak Gr_x dependence, equation (13) states that u_0 only depends on ζ in the lower part of the outer layer. With a reasonable accuracy we were able to fit the coefficients in equation (13) with the existing velocity data (which were all obtained not too far from $Gr_x = 10^{11}$, see Fig. 1(a)) by

$$\frac{u}{u_0} = 4.34 \ln \zeta - 3.13\zeta + 0.57\zeta \ln \zeta + 24.3. \tag{23}$$

The numerical results for increasing Gr_x in Fig. 8(b) show that u/u_0 and ζ are not properly scaled in the (lower part of the) outer layer; according to the numerical results, equation (23) describes the velocity only close to $Gr_x = 10^{11}$, but it is not a wall function. Cheesewright's assumption of negligible convection in the (lower part of the) outer layer might account for this discrepancy.

5. PRACTICAL USE OF WALL FUNCTIONS

In the preceding we have verified the existence of the following similarity shapes in the natural convection boundary layer for air (with a fixed Prandtl number of 0.71):

inner layer

$$\frac{u}{u_\tau} = f\left(\frac{y}{x} Gr_x^{1/4}\right) \tag{24a}$$

$$\frac{T-T_\infty}{\Delta T} = f(\zeta); \tag{24b}$$

buoyant sublayer (wall function)

$$\frac{u-u_0^3}{u_\tau^4} = f\left(\frac{yg\beta\Delta T}{u_\tau^2}\right) \tag{25a}$$

$$\frac{T-T_\infty}{\Delta T} = c_3 \zeta^{-1/3} + c_4; \tag{25b}$$

outer layer (defect laws)

$$\frac{u-u_{\max}}{u_0 \zeta_\delta^{1/3}} = f\left(\frac{y}{\delta}\right)$$

$$\left(\frac{T-T_\infty}{\Delta T}\right)\frac{Gr_\delta^{1/3}}{\zeta_\delta^{2/3}} = f\left(\frac{y}{\delta}\right). \tag{26}$$

Equation (25a) is found from equation (24a) after substitution of the wall-shear stress law $c_{fx} \div Gr_x^{-1/4}$ (equation (15) or (16)).

For comparison, the similarity shapes for a forced convection boundary layer are:

inner layer

$$\frac{u}{u_\tau} = f(y^+); \tag{27}$$

inertial sublayer (wall function)

$$\frac{u}{u_\tau} = c_5 \ln (y^+) + c_6; \tag{28}$$

outer layer (defect law)

$$\frac{u_\infty - u}{u_\tau} = f\left(\frac{y}{\delta}\right). \tag{29}$$

The wall functions for the forced and natural convection flow hold for equilibrium flows: no pressure gradient along the outer edge in the case of forced convection and no stratification along the outer edge in the case of natural convection. In computational practice, wall functions are used as boundary conditions to calculate non-equilibrium flows. For example, the forced convection flow in an enclosure can be calculated by solving the time-averaged Navier–

Stokes equations, using a k–ε model for the turbulence. At the first computational grid point from the wall the logarithmic wall function (28) is applied. This wall function has one degree of freedom, namely u_τ; its value is calculated by smoothly matching the wall function to the numerical solution. In a natural convection calculation in an enclosure, differentially heated over the vertical sides, one might use George and Capp's temperature wall function (25b). This wall function has two degrees of freedom, namely T_∞ and the wall-heat transfer $[\partial T/\partial y]_w$ appearing in the ζ coordinate. The wall function for the velocity, equation (25a), as found in this numerical study, also has two degrees of freedom T_∞ (or ΔT) and u_τ.

There are two remarkable differences between the wall functions for the forced and natural convection boundary layer.

(1) The inertial sublayer is fully turbulent, whereas the turbulent viscosity is very small in the buoyant sublayer.

(2) The log-law in the inertial sublayer gives a good approximation until close to the outer edge ($y^+ > 1000$), while the extension of the buoyant sublayer is restricted to the velocity maximum at $\zeta \sim 1.0$, which corresponds to $y^+ \sim 25$ (we have taken $Gr_x = 10^{11}$).

Because of the last difference, the application of wall functions in natural convection calculations can save only a few computational grid points in comparison with forced convection calculations. In natural convection calculations it seems to be more logical to use the defect laws, equations (26), as boundary conditions. This is because in natural convection the defect law turns out to be the similarity function over most of the boundary-layer thickness. Unfortunately these defect laws have more degrees of freedom, namely u_{max}, T_∞, δ and the wall-heat transfer $[\partial T/\partial y]_w$ appearing in ζ. This will complicate the matching between the wall function and the numerical solution.

Therefore, the practical use of similarity functions in natural convection flows is much less straightforward than in forced convection flows. Much research is still required to establish their practical value. At the moment we suggest that it is safer to calculate natural convection flows up to the wall with a low-Reynolds number k–ε model for turbulence, instead of using similarity functions.

6. CONCLUSION

By numerically solving the boundary-layer equations for air, with different low-Reynolds number k–ε models for the turbulence, the similarity scalings for the turbulent natural convection boundary layer along a heated vertical plate were derived. Some scalings (giving wall functions and defect laws) agree with the analytical results of George and Capp, others do not. All the turbulence models approximately predict the same scalings, i.e. characteristic quantities can be fitted to $\propto Gr_x^\gamma$ for large Grashof numbers, in which γ is almost independent of the model.

The inner layer, in which the turbulent viscosity is negligibly small, extends from the wall up to the velocity maximum. The calculations show that the wall-shear stress and wall-heat transfer behave as $c_{fx} \div Gr_x^{-1/4}$ and $Nu_x \div Gr_x^{1/3}$, respectively. Both powers agree with experiments. The power for the wall-heat transfer agrees with the theory of George and Capp, but the power for the wall-shear stress does not: they found $-1/3$ instead of $-1/4$. The numerical results show that the velocity profile scales with the laminar scalings in the conductive/thermo-viscous sublayer; $u_b = \sqrt{(g\beta\Delta T x)}$ for the velocity and $x\,Gr_x^{-1/4}$ for the length. On the contrary, for the temperature $(T-T_\infty)/\Delta T$ the similarity length is $\zeta = (y\ Nu_x)/x\ (\div y/(x\,Gr_x^{-1/3}))$. The buoyant sublayer is the intermediate layer between the conductive/thermo-viscous sublayer and the outer layer. George and Capp's wall function in the buoyant sublayer for the temperature is confirmed by the numerical results. Their wall function in the buoyant sublayer for the velocity is not found; we calculate that the laminar scalings u_b and $x\,Gr_x^{-1/4}$ are the right scalings, instead of their velocity $u_0 = (g\beta\Delta T\nu)^{1/3}$ and coordinate ζ.

The outer layer extends from the velocity maximum up to the edge of the boundary layer. In this layer the turbulent viscosity grows from almost zero at the velocity maximum, reaches a maximum and falls back to zero at the outer edge. The length scale δ is calculated to be almost independent of Gr_x, namely $\delta \div x$. George and Capp's defect laws for the velocity and the temperature agree perfectly with the calculations. In particular the velocity scale is $u_b\,Gr_x^{-1/18}$, which is close to the laminar velocity scale u_b as found numerically in the inner layer. Therefore, the laminar velocity scale is approximately the right velocity scale over the whole thickness of the boundary layer. Using the outer length scale x and the velocity scale u_{max} (which is close to the outer scaling $u_b\,Gr_x^{-1/18}$) leads to the best similarity profiles (defect laws) for the turbulent quantities ν_t, k and ε. Cheesewright's wall function for the temperature in the (lower part of the) outer layer can only be approximately recognized in the numerical results. His wall function for the velocity disagrees with the computational results.

REFERENCES

1. W. K. George and S. P. Capp, A theory for natural convection turbulent boundary layers next to heated surfaces, *Int. J. Heat Mass Transfer* **22**, 813–826 (1979).
2. R. Cheesewright, The scaling of turbulent natural convection boundary layers in the asymptotic limit of infinite Grashof number, paper presented at Euromech Colloquium 207, 7–9 April, Delft, The Netherlands (1986).
3. R. Cheesewright and M. H. Mirzai, The correlation of experimental velocity and temperature data for a turbulent natural convection boundary layer, *Proc. 2nd*

U.K. Natn. Conf. on Heat Transfer, Glasgow, pp. 79–89 (1988).
4. T. Tsuji and Y. Nagano, Characteristics of a turbulent natural convection boundary layer along a vertical flat plate, *Int. J. Heat Mass Transfer* **31**, 1723–1734 (1988).
5. R. Cheesewright, Turbulent natural convection from a vertical plane surface, *J. Heat Transfer* **90**, 1–8 (1968).
6. R. Cheesewright and E. Ierokipiotis, Velocity measurements in a natural convection boundary layer, Queen Mary College, Faculty of Engineering Research, Report EP 5022, London (1981).
7. R. Cheesewright and E. Ierokipiotis, Velocity measurements in a turbulent natural convection boundary layer, *Proc. 7th Int. Heat Transfer Conf.*, Munich, Vol. 2, pp. 305–309 (1982).
8. M. Miyamoto, H. Kajino, J. Kurima and I. Takanami, Development of turbulence characteristics in a vertical free convection boundary layer, *Proc. 7th Int. Heat Transfer Conf.*, Munich, Vol. 2, pp. 323–328 (1982).
9. M. Miyamoto, Y. Katoh, J. Kurima and H. Kajino, An experimental study of turbulent free convection boundary layer along a vertical surface using LDV, *Proc. Osaka Symp.*, 15 July, Osaka, Japan, pp. 83–104 (1983).
10. D. L. Siebers, R. F. Moffatt and R. G. Schwind, Experimental, variable properties natural convection from a large, vertical flat surface, *J. Heat Transfer* **107**, 124–132 (1985).
11. S. Ostrach, An analysis of laminar free-convection flow and heat transfer about a flat plate parallel to the direction of the generating body force, NACA Report 1111 (1953).
12. T. Cebeci and P. Bradshaw, *Physical and Computational Aspects of Convective Heat Transfer*. Springer, Berlin (1984).
13. R. A. W. M. Henkes and C. J. Hoogendoorn, Comparison of turbulence models for the natural convection boundary layer along a heated vertical plate, *Int. J. Heat Mass Transfer* **32**, 157–169 (1989).
14. W. P. Jones and B. E. Launder, The prediction of laminarization with a two-equation model of turbulence, *Int. J. Heat Mass Transfer* **15**, 301–314 (1972).
15. K.-Y. Chien, Predictions of channel and boundary layer flows with a low-Reynolds-number two-equation model of turbulence, AIAA-80-0134 (1980).
16. K.-Y. Chien, Predictions of channel and boundary-layer flows with a low-Reynolds-number turbulence model, *AIAA J.* **20**, 33–38 (1982).
17. C. K. G. Lam and K. Bremhorst, A modified form of the k–ε model for predicting wall turbulence, *J. Fluids Engng* **103**, 456–460 (1981).

DETERMINATION NUMERIQUE DES FONCTIONS DE PAROI POUR LA COUCHE LIMITE TURBULENTE DE CONVECTION NATURELLE

Résumé—Par une voie analytique, George et Capp (*Int. J. Heat Mass Transfer* **22**, 813–826 (1979)) et Cheesewright ("Couches limites turbulentes de convection laminaire asymptotiques à nombre de Grashof infini", présenté au colloque Euromech 207 (1986)) ont obtenu des fonctions de paroi pour la couche limite laminaire le long d'une plaque chaude verticale. On compare ici ces fonctions à des calculs numériques pour l'air avec le modèle k–ε modifié pour un faible nombre de Reynolds. La fonction de paroi pour la température dans la couche interne de George et Capp s'accorde bien avec les calculs mais pas la fonction de paroi pour la vitesse. On retrouve numériquement les lois déficitaires de George et Capp pour la vitesse et la température dans la couche externe, mais la fonction de paroi de Cheesewright pour la vitesse ne convient pas pour la partie basse de la couche externe.

NUMERISCHE BESTIMMUNG VON WANDFUNKTIONEN FÜR DIE GRENZSCHICHT IN TURBULENTER NATÜRLICHER KONVEKTION

Zusammenfassung—George und Capp (*Int. J. Heat Mass Transfer* **22**, 813–826 (1979)) sowie Cheesewright (Euromech Colloquium 207 (1986)) haben Wandfunktionen für die Grenzschicht bei natürlicher Konvektion an einer beheizten senkrechten Platte entwickelt. Diese Funktionen werden hier mit numerischen Berechnungen für Luft verglichen, wobei ein für kleine Reynolds-Zahlen modifiziertes k–ε-Turbulenzmodell angewandt wird. Die Wandfunktion nach George und Capp für die Temperatur der inneren Schicht stimmt gut mit den Berechnungen überein, dies gilt jedoch nicht für ihre Wandfunktion für die Geschwindigkeit. Die Gesetzmäßigkeiten von George und Capp für die Geschwindigkeit und die Temperatur in der äußeren Schicht wurden enbenfalls numerisch bestätigt, hingegen ergab sich für die Wandfunktion der Geschwindigkeit nach Cheesewright für den unteren Teil der äußeren Schicht keine Übereinstimmung.

ЧИСЛЕННОЕ ОПРЕДЕЛЕНИЕ ФУНКЦИЙ СТЕНКИ ДЛЯ ТУРБУЛЕНТНОГО ЕСТЕСТВЕННОКОНВЕКТИВНОГО ПОГРАНИЧНОГО СЛОЯ

Аннотация—Джордж и Кэпп (*Int. J. Heat Mass Transfer* **22**, 813–826 (1979)), а также Чизрайт ("The scaling of turbulent natural convection boundary layers in the asymptotic limit of infinite Grashof number", доклад, представленный на Euromech Colloquium 207 (1986)) вывели аналитическим способом функции стенки для естественноконвективного пограничного слоя вдоль нагретой вертикальной пластины. В данной работе эти функции сравниваются с численными расчетами для воздуха, выполненными на основе k–ε модели турбулентности с модификациями при низких числах Рейнольдса. Выведенные Джорджем и Кэппом функции стенки для температуры во внутреннем слое хорошо согласуются с расчетами, в отличие от функции стенки для скорости. Численно определены описанные Джорджем и Кэппом законы для скорости и температуры во внешнем слое, однако функция стенки, полученная Чизрайтом для скорости в нижней части внешнего слоя, не согласуется с расчетами.